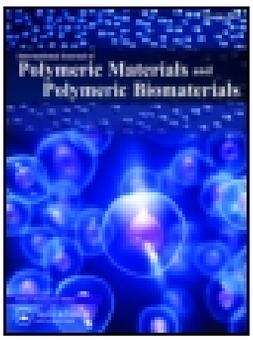

International Journal of Polymeric Materials and Polymeric Biomaterials

ISSN: (Print) (Online) Journal homepage: https://www.tandfonline.com/loi/gpom20

Lipid-polymer hybrid nanoparticles as a targeted drug delivery system for melanoma treatment

Rodrigo Scopel, Manuel A. Falcão, Angélica Regina Cappellari, Fernanda B. Morrone, Silvia S. Guterres, Eduardo Cassel, Andrea M. Kasko & Rubem M. F. Vargas

To cite this article: Rodrigo Scopel, Manuel A. Falcão, Angélica Regina Cappellari, Fernanda B. Morrone, Silvia S. Guterres, Eduardo Cassel, Andrea M. Kasko & Rubem M. F. Vargas (2020): Lipid-polymer hybrid nanoparticles as a targeted drug delivery system for melanoma treatment, International Journal of Polymeric Materials and Polymeric Biomaterials, DOI: 10.1080/00914037.2020.1809406

To link to this article: https://doi.org/10.1080/00914037.2020.1809406

INTERNATIONAL JOURNAL OF POLYMERIC MATERIALS AND POLYMERIC BIOMATERIALS
https://doi.org/10.1080/00914037.2020.1809406

Lipid-polymer hybrid nanoparticles as a targeted drug delivery system for melanoma treatment

Rodrigo Scopel[a], Manuel A. Falcão[a], Angélica Regina Cappellari[b], Fernanda B. Morrone[b], Silvia S. Guterres[c], Eduardo Cassel[a], Andrea M. Kasko[d,e], and Rubem M. F. Vargas[a]

[a]Faculdade de Engenharia, Laboratório de Operações Unitárias, Pontifícia Universidade Católica do Rio Grande do Sul, Porto Alegre, Brazil; [b]Laboratório de Farmacologia Aplicada, Pontifícia Universidade Católica do Rio Grande do Sul, Porto Alegre, Brazil; [c]Programa de Pós-Graduação em Ciências Farmacêuticas, Faculdade de Farmácia, Universidade Federal do Rio Grande do Sul, Porto Alegre, Brazil; [d]Department of Bioengineering, University of California, Los Angeles, California, USA; [e]California Nanosystems Institute, Los Angeles, California, USA

ABSTRACT

Aiming to target vitamin D receptors (VDR) expressed in melanoma cells, vitamin D_3 functionalized hybrid lipid-polymer nanoparticles (HNP-VDs) comprising a poly(lactic-co-glycolic acid) (PLGA) core and a lipid shell composed of hydrogenated soy phosphatidylcholine (HSPC), cholesterol (CHOL) and 1,2-disteroyl-sn-glycero-3-phosphaethanolamine-N[succinyl(polyethyleneglycol)-2000 (DSPE-PEG_{2000}) were synthesized. The nanocarriers were optimized to a lipid surface area coverage of 97%. *In vitro* drug release studies showed an initial burst release in the first 24 h followed by diffusive transport. Finally, cellular uptake experiments demonstrated that the HNP-VDs efficiently targeted B16 melanoma cells, thus resulting in a promising vehicle to deliver therapeutics for the melanoma treatment.

GRAPHICAL ABSTRACT

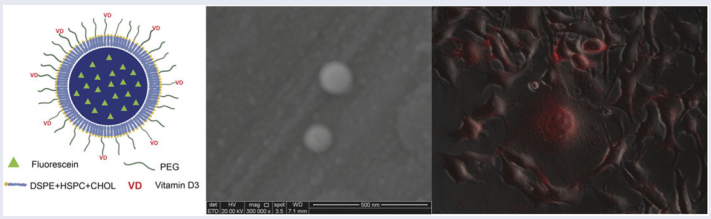

ARTICLE HISTORY
Received 12 December 2019
Accepted 10 August 2020

KEYWORDS
Controlled release; drug delivery systems; lipid-polymer hybrid nanoparticles; melanoma; vitamin D receptor

1. Introduction

Nanocarriers designed for the delivery of therapeutics have been widely studied in pharmaceutical and biomedical applications enabling targeted delivery to site of action, resulting in higher therapeutic efficacy[1–3]. Liposomes and polymeric nanoparticles are the most widely adopted nanosystems for drug delivery[4–8] among nanoparticle-based therapeutics. Polymeric nanoparticles exhibit excellent drug loading and stability but present lower biocompatibility. In contrast, liposomes exhibit excellent biocompatibility, even though they suffer from drug leakage and instability during storage[9, 10]. In order to overcome the disadvantages of both types of nanoparticles, many research groups have focused their efforts on the development of hybrid systems that combine the biomimetic characteristics of the liposomes and the stability of polymeric nanoparticles[11]. In the past decade, these lipid-polymer hybrid nanoparticles (HNPs) have been increasingly recognized as promising drug delivery vehicles due to their multiple advantageous features[12]. From the structural point of view, these particles consist of a polymeric core coated with single or multiple layers of lipids that constitute the shell.

Poly(lactic-co-glycolic acid) (PLGA) has been exploited widely in the design of nanoparticles due to its safe drug release profile, biocompatibility, biodegradability and protection of drug molecules from degradation[13, 14]. Moreover, clinical products made from this copolymer have been approved by the US Food and Drug Administration (FDA) to deliver therapeutics (i.e., Eligard® and Zoladex®). As a result of these factors, PLGA has also been studied for the development of HNPs[5]. For example, Palange et al.[15] fabricated nanoparticles using PLGA as the polymeric core and two lipids, 1,2-dipalmitoyl-sn-glycero-3-phosphocoline (DPPC) and DSPE-PEG_{2000}, as the lipid shell surrounding the particles. The authors encapsulated the natural anti-inflammatory compound curcumin and demonstrated the firm arrest of circulating breast cancer cells (MDA-MB-231)

CONTACT Rubem M. F. Varga rvargas@pucrs.br Faculdade de Engenharia, Laboratório de Operações Unitárias, Pontifícia Universidade Católica do Rio Grande do Sul Av. Ipiranga 6681 Pr. 30 S. 208-F. Porto Alegre, 90619-900, Brazil.

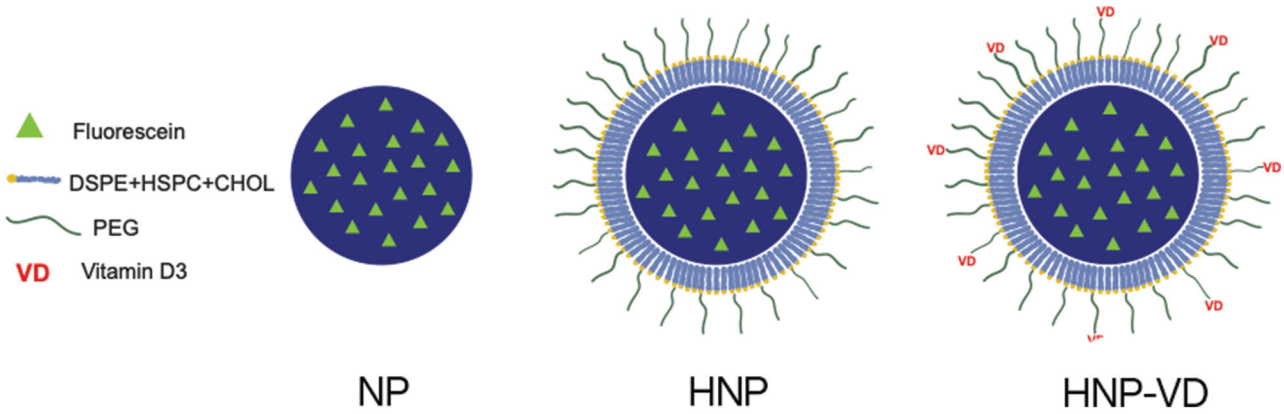

Figure 1. PLGA nanoparticle (NP) – hybrid lipid-polymer nanoparticle (HNP) – vitamin D3 functionalized hybrid lipid-polymer nanoparticle (HNP-VD).

onto inflamed endothelium. Hu et al.[16] produced hybrid lipid-PLGA nanoparticles of various cholesterol (CHOL) concentrations to evaluate its influence over the stability of long-term stored HNPs, the release of a model antigen (bovine serum albumin – BSA) in human serum and PBS buffer, and their *in vitro* uptake by dendritic cells. The authors demonstrated that increasing the content of CHOL in the lipid layer extended the release of the antigen *in vitro*, facilitated uptake, and protected the integrity of the hybrid nanostructure.

Aiming to increase the efficacy of the HNPs, ligands can be conjugated onto their surface in order to target specific receptors. In the work by Zhao et al.[9], HNPs functionalized with folic acid were developed for the release of paclitaxel against cervical cancer cells. The folate functionalized HNPs resulted in better tumor size reduction and increased life expectancy in mice, compared to free paclitaxel.

Mo et al.[17] investigated three types of particle formulation with the goal of improving drug delivery. The authors suggested that PEGylated hyaluronic acid-coated liposomes with narrow size distribution and high encapsulation efficiency has affectivity for the tumor-targeted delivery of the antineoplastic drug sorafenib.

Preclinical studies have demonstrated that several melanoma cell lines express the vitamin D receptor (VDR)[18, 19]. Slominski et al.[20] have tested two hydroxyvitamin D_3 analogs aiming to understand their activity on normal and malignant melanocytes. The authors concluded that both molecules inhibited proliferation and colony formation by melanoma cells. These effects were correlated with ligand-induced translocation of VDR to the nucleus, thus, qualifying the receptor as a promising strategy and potential candidate for the development of a targeted drug delivery system for malignant melanoma treatment.

As far as the authors are concerned, this is the first study to investigate the use of the vitamin D receptor as a targeting moiety for nanocarriers. Therefore, the objective of this work was the synthesis of HNPs composed of a PLGA core and a lipid mixture – hydrogenated soy phosphatidylcholine (HSPC), CHOL and DSPE-PEG_{2000} – as a shell. Aiming to target the VDR and increase cell internalization, vitamin D_3 functionalized lipid-polymer hybrid nanoparticle (HNP-VD) were also produced by using vitamin D_3 covalently bound to DSPE-PEG_{2000}. B16 mouse melanoma cells are among the cell lines that express the VDR and, therefore, were used as a model for *In vitro* cell viability and cellular uptake assessments[21].

2. Materials and methods

Poly(lactic-co-glycolic acid) (PLGA — 50:50) was donated by PURAC (Germany). The solvents ethyl acetate (EtAc), dichloromethane (DCM) and dimethyl sulfoxide (DMSO) were purchased from Merck (Germany). Poly(vinyl alcohol) (PVA), fluorescein, trehalose, cholesterol (CHOL), iron (III) chloride hexahydrate and ammonium thiocyanate were obtained from Sigma-Aldrich (Germany). Chloroform was obtained from Fisher Scientific (USA). For the synthesis of the HNPs, hydrogenated soy phosphatidylcholine (HSPC), 1,2-disteroyl-sn-glycero-3-phosphaethanolamine-*N*-[succinyl(polyethylene glycol)-2000 (DSPE-PEG_{2000}) and 1,2-distearoyl-sn-glycero-3-phosphoethanolamine-*N*-[cholecalciferol(polyethylene glycol)-2000] (DSPE-PEG_{2000}-VD) were purchased from Nanosoft Polymers. In addition, all reagents for cell culture were purchased from Gibco/Invitrogen (Life Technologies - Carlsbad, CA, United States).

2.1. Synthesis of PLGA nanoparticles

The synthesis of polymeric nanoparticles (NP), lipid-polymer hybrid nanoparticles (HNP) and functionalized lipid-polymer hybrid nanoparticles (HNP-VD) (Figure 1) were carried out according to the following procedures.

The synthesis of the PLGA NPs was carried out using the solvent evaporation emulsification method[22]. For each sample, 50 mg of PLGA were weighed and dissolved in 1 mL of a EtAc:DMSO (3:1) solution. Samples containing fluorescein and Nile red were prepared by dissolving 1.25 mg and 0.5 mg in the solvent phase, respectively. Two aqueous solutions of PVA (0.3 and 3.0% *w/v*) were prepared and 25 mL of the 0.3% (*w/v*) solution was transferred into a 50 mL beaker and agitated (250 rpm). 2 mL of the 3.0% (*w/v*) solution was added to a 15 mL centrifuge tube. Subsequently, the PLGA solution was added dropwise to the centrifuge tube under vigorous vortexing. Once the entire volume was added, 30 seconds of additional vortexing was conducted.

Table 1. Equivalents used in the synthesis of the HNPs for different lipid: NPs ratios.

Mass ratio (Lipid:NPs)	Molar ratio	M_w (g/mol)	mg	mmol
1:1				
HSPC	2	785	20.8	0.02650
CHOL	1	387	5.1	0.01320
DSPE-PEG_{2000}	0.1	2993	4.1	0.00140
1:10				
HSPC	2	785	1.92	0.00240
CHOL	1	387	0.52	0.00130
DSPE-PEG_{2000}	0.1	2993	0.40	0.00010
1:20				
HSPC	2	785	1.06	0.00130
CHOL	1	387	0.27	0.00070
DSPE-PEG_{2000}	0.1	2993	0.20	0.00007
1:25				
HSPC	2	785	0.70	0.00090
CHOL	1	387	0.20	0.00040
DSPE-PEG_{2000}	0.1	2993	0.10	0.00004

Afterward, the centrifuge tube was placed on an ice bath and transferred to a probe ultrasonicator for 30 seconds (60% amplitude and 8 W). This process (vortex − 30 s/ultrasonicator − 30 s) was repeated three times. Finally, the dispersion was transferred to the 0.3% (*w/v*) PVA solution where the nanoparticles were allowed to harden for 12 h. NPs collection was conducted by transferring the dispersion to an Oak Ridge tube and centrifuging at 25,000 rcf for 60 min. After, the supernatant was discarded and the particles were resuspended in deionized water. This washing step was repeated three times. The NPs were then resuspended in a trehalose:polymer (1:2) solution, frozen in liquid nitrogen and lyophilized for 72 h.

2.2. Synthesis of hybrid lipid-polymer nanoparticles (HNPs)

HNPs were synthesized using the gentle hydration method[9, 23–25]. This method consists of the formation of a lipid thin film in a round bottom flask followed by the hydration of this layer by a dispersion of NPs. In this work, the hybrid NPs were produced with and without the presence of targeting ligands. Briefly, a mixture of lipids[26] HSPC:CHOL:DSPE-PEG_{2000} (2:1:0.1 molar ratio) was dissolved in 5 mL of $CHCl_3$. Subsequently, the solvent was evaporated using a rotary evaporator, creating a thin lipid film on the wall of the round bottom flask. The NPs previously prepared were resuspended in 5 mL of deionized water (6 mg/mL), added to the round bottom flask containing the lipid film at 1 mL/min and sonicated for 10 min. The round bottom flask was transferred to a stirring plate and the HNPs were left to self-assemble for 30 min under gentle stirring and then lyophilized.

The HNPs containing the targeting ligand (HNP-VD) were prepared using the same method, however, the mixture of lipids was substituted by HSPC:CHOL:DSPE-PEG_{2000}:DSPE-PEG_{2000}-VD (2:1:0.08:0.02 molar ratio).

Additionally, aiming to optimize the amount of lipids used in the synthesis, HNPs were prepared using the following lipid: NPs ratios: 1:1, 1:10, 1:20 and 1:25 (*w/w*). Table 1 presents the quantities used for different samples.

2.3. Characterization of the nanoparticles

The NPs and HNPs were characterized by field emission scanning electron microscopy (FEG-SEM), dynamic light scattering (DLS) and zeta potential[27]. Microscopy analysis were performed on the equipment Fei® Inspect F50. The images were obtained applying a drop of an aqueous solution of NPs or HNPs (100 µg/mL) directly to the top of the stub. Subsequently, the samples were subjected to gold sputtering for 80 seconds. The parameters for the visualization of particles were: distance of 7–8 mm, 20 kV and magnification of 70,000–300,000×. The determination of the hydrodynamic diameter, performed by DLS, as well as the zeta potential analysis, were conducted on the ZetaSizer® Nanoseries equipment (Malvern, England).

2.4. Quantification of lipid surface coverage

The method of quantification of lipids on the surface of HNPs, described by Yang et al.[28], is based on two analysis. First, a colorimetric assay was used in which the formation of complexes of phospholipids with ammonium ferrothiocyanate are quantified[29]. Second, a ^{1}H-NMR analysis is performed to quantify the amount of DSPE-PEG_{2000} present on the surface of the HNPs from the proton absorptions of lactate units (5.19 ppm), glycolate units (4.91 ppm) and ethylene oxide units (3.51 ppm).

The first method was applied by dissolving 2 mg of HNPs produced with different polymer/lipid ratios (1:1, 1:10, 1:20, 1:25 *w/w*) in $CHCl_3$. The resulting solution was mixed with 2 mL of the ammonium ferrothiocyanate solution and subsequently vortexed (60 s) to form the complex. The resulting mixture was centrifuged at low speed and the absorbance of HSPC/AF complexes were measured at the wavelength of 471 nm. The amount of lipids was calculated using a standard curve previously prepared with the same lipid composition of the shell of the HNPs.

The standard solution of ammonium ferrothiocyanate was prepared according to Stewart[29]. Briefly, 27.03 g of iron (III) chloride hexahydrate and 30.4 g of ammonium thiocyanate were dissolved in 1 L of deionized water. Subsequently, a 2:1:1 (molar ratio) mixture of HSPC, CHOL and DSPE-PEG_{2000} was dissolved in 100 mL $CHCl_3$. Volumes between 0.1 and 1.0 mL of this solution were added to 2 mL of the ammonium ferrothiocyanate solution in a centrifuge tube and sufficient $CHCl_3$ was added to bring the final volume to 4 mL. The system was vortexed for 1 minute, the organic phase removed using a Pasteur pipette and then added to a cuvette for absorbance analysis via UV/Vis ($\lambda = 471$ nm).

From the values obtained, the amount of lipids per milligram of HNPs, the number of lipids per HNPs and the percentage of coating of HNPs can be calculated by Eqs.1–3, respectively.

$$V_1 = \frac{M_L/Mw_L}{M_{NP_s}} \quad (1)$$

$$V_2 = V_1 \; N_A V_{NPs} \; \rho_{PLGA} \quad (2)$$

$$V_3 = \frac{V_2 S_L}{S_i} \times 100\% \quad (3)$$

Where V_1 is the number of moles of lipids per mg of HNP, V_2 is the number of lipids per HNP and V_3 is the percentage of coating of the HNP. M_L is the mass of lipids used in the preparation of HNP, M_{NPs} is the mass of nanoparticles analyzed, Mw_L is the molecular weight of lipids, V_{NPs} is the individual volume of each NP, ρ_{PLGA} is the density of PLGA and N_A is the Avogadro number. S_i is the surface area of a single NP and S_L is the area of the polar portion of the HSPC and DSPE-PEG$_{2000}$ molecules which, as reported by Yang et al.[28], are given by 0.694 nm^2 and 1.240 nm^2, respectively.

2.5. Drug release study

In this work, the release of the model drug fluorescein from NPs, HNPs and HNP-VDs were performed in triplicate using the dialysis method for 6 days[30]. For each experiment, 5 mg of sample were dispersed in 1 mL of the release medium (PBS, pH 7.4, 0.01 M) and placed in contact with the dialysis membranes (M_w cutoff = 14,000 Da) in the Franz cell donor compartment (Automated Franz Cells – Microette Plus, Hanson Research Corporation, USA). The receiver compartment, where 7 mL of the release medium were placed, was maintained under constant stirring at a temperature of 32 °C. At pre-determined intervals (0.5, 1, 2, 4, 8, 12, 24, 48, 72, 96, 120 and 144 h), 1 mL aliquot was withdrawn from the recipient medium and the same volume of PBS added to maintain the infinite dilution condition. Analysis of samples taken at different times were performed by spectrofluorimetry in a plate reader (Molecular Devices – SpectraMax M2e).

In order to obtain the encapsulation efficiency (EE) and drug loading efficiency (DL), the methodology presented by Hara et al.[31] was used and their values can be calculated according to Eqs. 4 and 5. Briefly, 2 mg of fluorescein-loaded nanoparticles were dissolved in 1 mL of acetonitrile and added to 10 mL of PBS in order to separate the PLGA from the fluorescein. Subsequently, the PLGA was filtered through a cellulose filter (pore size: 0.2 µm) and the solution analyzed by UV/Vis at a fixed wavelength ($\lambda = 490$ nm). The concentration of fluorescein present in the analyzed nanoparticles was then calculated from a calibration curve.

$$EE = \frac{\text{weight of drug in NPs}}{\text{weight of drug added}} \times 100\% \quad (4)$$

$$DL = \frac{\text{weight of drug in NPs}}{\text{weight of NPs}} \times 100\% \quad (5)$$

2.6. Cell culture

B16 cell line, representative of mouse melanoma, was purchased from the American Cell Culture Collection (ATCC). Cells were grown in Dulbecco's Modified Eagle Medium supplemented with 10% fetal bovine serum (FBS), penicillin/streptomycin (100 U/mL) and fungizone. In addition, the cells were maintained at the temperature of 37 °C, 95% air humidity and 5% CO_2.

2.7. In vitro cell viability assay

The evaluation of cell viability was performed as described by Gehring et al.[32] using B16 melanoma cells. Briefly, 6.5×10^3 cells were seeded in 96-well plates and maintained under optimal culture conditions until reaching 70% confluence. After this period, the cells were treated with different concentrations of nanoparticles (10, 50, 100 and 500 µg/mL) previously filtered (0.45 µm filter) in their different NP, HNP and HNP-VD formulations. Cells were maintained 24 h after treatment and afterwards they were submitted to cell viability analysis. Firstly, cells were washed with PBS and incubated with a solution of 3-(4,5-dimethylthiazol-2-yl)-2,5-diphenyltetrazolium bromide (MTT) (Sigma Aldrich, Inc.) (5 mg/mL) diluted in DMEM 10% of FBS. The crystals of formazam, a product of the mitochondrial oxidation-reduction reaction of viable cells, were dissolved in 100 µL of dimethylsulfoxide (DMSO), and the staining intensity was determined by the SpectraMax M2e-Molecular Devices equipment at $\lambda = 570$ nm. The absorbance was directly proportional to the number of living cells with active mitochondria. The results were expressed as percentage in relation to the control without treatment.

2.8. Cellular uptake

In order to evaluate the cellular uptake of the nanoparticles, B16 melanoma cells were treated with the different formulations containing the fluorescent marker Nile red (NR). Cells (2.0×10^4) were seeded in 24-well plates and incubated under ideal conditions of cultivation for 24 hours. After, cells were treated for 3 hours with NP, HNP and HNP-VD, containing NR, at the concentrations of 50 and 100 µg/mL. Then, the culture medium was removed, the cells were washed three times with PBS and analyzed via inverted fluorescence microscopy (Olympus IX71®).

2.9. Statistical analysis

For the evaluation of the results, the ANOVA one-way test was used, followed by Tukey post-hoc test. The results were expressed as mean ± standard error. The GraphPad Prism 5.0® program was used to evaluate the results and also to generate the graphs. $p < 0.05$ was considered significant.

3. Results and discussion

3.1. Synthesis of NP, HNP and HNP-VD

PLGA nanoparticles (NPs) were prepared by the simple emulsification/solvent evaporation method. This methodology is widely reported in the literature for the production of polymeric NPs for different applications[22, 25, 33, 34]. The NPs were produced with properties such as size, zeta

potential and polydispersity index (PDI) suitable for application in drug delivery systems (Table 2). Among these properties, the low PDI (<0.1) was observed, confirming the homogeneity of the sample size distribution. From the images obtained in the FEG-SEM (Figure 2) it is possible to verify the spherical morphology of the NPs as well as to confirm the size and the narrow distribution data observed via DLS.

As expected, an increase in the size of the NPs occurred after adding a lipid layer on its surface. The PDI also increased significantly. This may be due to the excess amount of phospholipids resulting in the formation of micelles with different sizes and without a polymeric core in the stage of synthesis of these particles. Therefore, the use of 1:1 mass ratio (lipids:NPs) may lead to a difficulty in the manufacturing step due to the possible simultaneous formation of lipid micelles. The zeta potential did not show any significant increase in its value after the introduction of the lipid layer. The negative charges are a consequence of the presence of terminal carboxyl groups in the polymer. According to Mandal et al.[11], the lipid-to-polymer ratio used in the synthesis of HNPs should be optimized since, when in excess, lipids may form micelles and liposomes absent of the polymeric core, which is consistent with our results. This fact can lead to aggregation and loss of active ingredients during the purification process[11, 35].

Table 2. NPs and HNPs characterization using the 1:1 lipid:NPs mass ratio.

Sample	Diameter (nm)	PdI	Zeta potential (mV)
NPs	133.6 ± 0.3	0.058 ± 0.012	−14.30 ± 0.70
NPHs	256.8 ± 38.4	0.286 ± 0.100	−13.59 ± 3.15

3.2. Optimization of lipid-to-polymer ratio

In order to avoid the formation of micelles without polymeric core and the excessive use of lipids to cover the HNPs, the coverage percentage of the lipid layer on the NPs

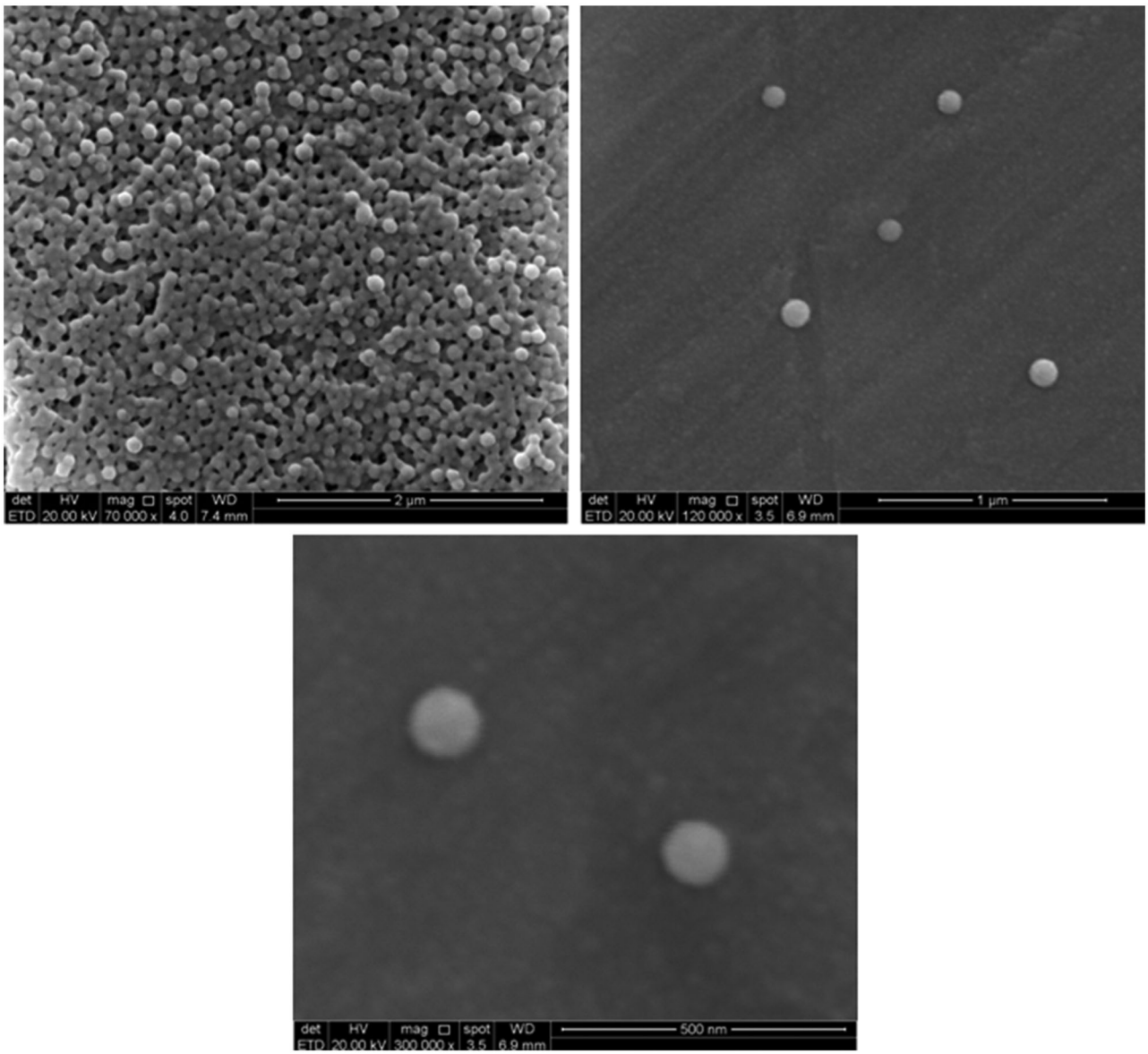

Figure 2. FEG-SEM images from the synthesized NPs at 70,000×, 120,000×, and 300,000×.

was quantified and the mass ratio (lipid:NPs) used in the synthesis was optimized using the following mass ratios: 1:10, 1:20 and 1:25 (*w/w*).

The HNPs were characterized as described previously for the NPs and the results obtained are summarized in Table 3. As the ratio of lipid:NP decreases, the particle size decreases, indicating that the lipid layer is less dense when less lipid is used to form the HNPs. The PDI was lower for particles formed with less lipid (1:10, 1:20 and 1:25) than those formed with the highest ratio (1:1). The lower PDI indicates that fewer, if any, lipid micelles may be forming. No significant change in zeta potential was observed when reducing the lipids:NPs mass ratio.

Table 3. HNPs characterization synthesized with different lipid: NPs mass ratio.

Lipid:NPs	Diameter (nm)	PdI	Zeta potential(mV)
1:1	256.77 ± 38.40	0.286 ± 0.10	−13.59 ± 3.15
1:10	209.80 ± 0.001	0.190 ± 0.19	−15.0 ± 1.56
1:20	189.30 ± 2.69	0.222 ± 0.08	−11.4 ± 2.19
1:25	163.20 ± 8.23	0.183 ± 0.01	−14.0 ± 1.30

The HNP coating percentage calculations can be performed from the colorimetric method presented by Stewart[29] together with ^{1}H-NMR analysis, as presented by Yang et al.[28]. The results of the ^{1}H-NMR analysis are presented in Figure 3, where the spectra provides the value of the proton integration of lactate, glycolate and ethylene oxide units. By calculating the ratio between these peaks, it is possible to quantify the percentage of DSPE-PEG$_{2000}$ in the sample. Analyzing the results, the ratios obtained were 1.93:1, 6.92:1, 10.9:1 and 12.7:1 for the mass ratios of 1: 1, 1:10, 1: 20 and 1:25, respectively. The values obtained for each compound relative to surface lipid density, molecules per NP and coating percentage are shown in Table 4.

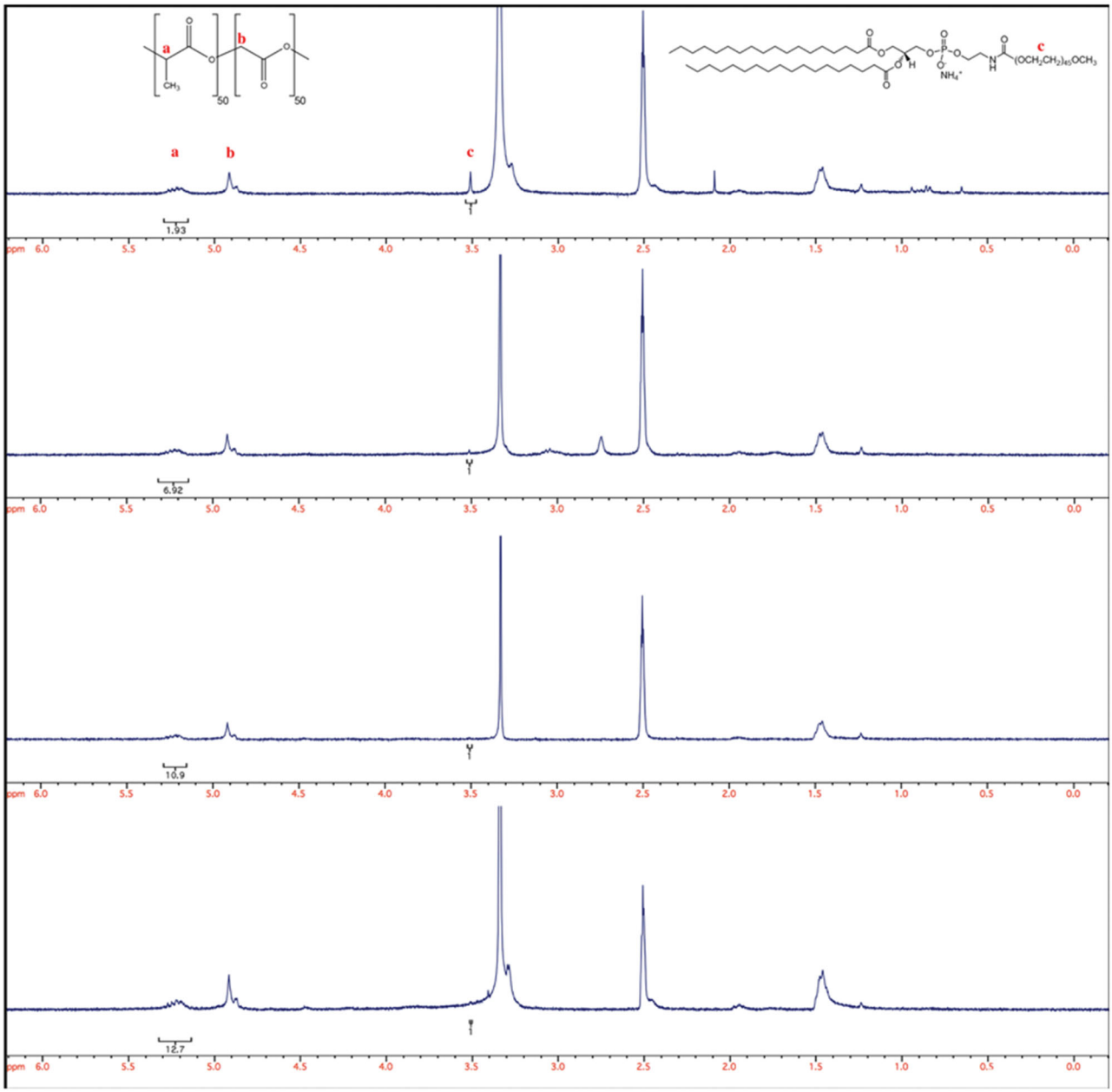

Figure 3. 1H-NMR spectra of HNPs synthesized. From top to bottom the lipid: NPs mass ratios of 1:1, 1:10, 1:20 and 1:25.

Table 4. Quantification of lipids on the surface of the HNPs.

	HSPC			$DSPE\text{-}PEG_{2000}$		
Lipid:NPs (*w/w*)	Surface density (nmol mg^{-1} NP)	Molecules per NP (10^4)	Coverage (%)	Surface density (nmol mg^{-1} NP)	Molecules per NP (10^4)	Coverage (%)
1:1	544.8 ± 15.0	554.1 ± 15.2	1394 ± 38	172.9	175.8	791
1:10	106.1 ± 3.1	50.2 ± 1.4	210 ± 6	48.3	22.9	171
1:20	62.7 ± 3.5	16.4 ± 0.9	102 ± 6	30.6	8.0	89
1:25	24.4 ± 1.6	3.8 ± 0.3	33 ± 2	26.2	4.1	64

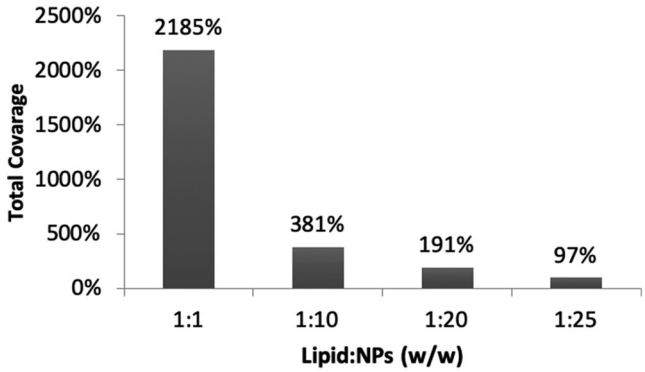

Figure 4. Total coverage of the NPs using different lipid:NPs ratios.

Table 5. NPs, HNPs, and HNP-VDs synthesized with the optimal conditions.

	Diameter (nm)	PDI	Zeta potential (mV)
NPs	133.6 ± 0.3	0.058 ± 0.012	−14.3 ± 0.7
NPHs	163.2 ± 6.7	0.184 ± 0.011	−14.0 ± 1.1
NPHs-F	175.4 ± 6.5	0.199 ± 0.011	−13.9 ± 0.1

The total coverage percentage is given by the sum of the partial coverages of HSPC and $DSPE\text{-}PEG_{2000}$. The total value for each mass ratios used in the HNPs preparations is shown in Figure 4.

As shown in Figure 4, the mass ratio of 1:25 exhibits a NP coating of 97% and, therefore, it was determined that this ratio is optimal for the production of HNPs and HNP-VDs. This condition is similar to the work presented by Desai et al.[10], where the authors used a 1:15 ratio, and Zhang et al.[36] where a ratio ranging from 10 to 20% was considered optimal. It is important to note that, in their work, the nanoprecipitation method for the synthesis of the hybrid NPs was used but the polymer was not PLGA. Those who performed the HNP preparation in two stages[9, 24, 25] used the ratio of 1:1, but do not state the percentage of area covered by the phospholipid layer.

All of the HNPs and HNP-VDs used subsequently in this work for drug release studies, *In vitro* cell viability and cellular uptake assessment were produced according to the optimized fabrication conditions (1:25 lipid:NPs mass ratio). The results obtained from the characterization of the nanocarriers synthesized with the optimal conditions are described in Table 5.

As expected, the diameter of the NPs increases when the phospholipid layer is introduced. Similarly, the HNPs that contain the vitamin D_3 ligand (HNP-VDs) are slightly larger than those without the ligand. However, zeta potential is unaffected by the addition of the ligand. Figure 5 shows the images obtained by FEG-SEM of the samples HNP and HNP-VD.

3.3. Drug release study

In order to perform release kinetics studies, NPs, HNPs and HNP-VDs containing fluorescein were fabricated and the release studies were conducted over six days. The amount of fluorophore encapsulated within each nanocarrier was quantified and the results are shown in Table 6.

In the first 24 h of incubation, 75, 62, and 57% of the fluorescein in the NPs, HNP, and HNP-VD were released respectively, configuring a burst release. For the subsequent period, a slower release was observed where the cumulative release of fluorescein from the NPs was 88%, 75% for the HNP and 68% for the HNP-VD (Figure 6). The release behavior is similar to the work presented by Zhao et al.[9] where the total percentage released from the NPs was the highest followed by HNP and HNP-VD. It is hypothesized that this occurs because introducing the lipid layer increases the diffusion distance of the fluorescein, as does adding the targeting ligand (according to nanoparticle diameters in Table 6). The lipid layer may also affect partitioning of the fluorescein within the nanoparticle, further hampering its release.

3.4. In vitro *cell viability*

In order to demonstrate the effect of the nanoparticles on cell viability, the different formulations (NP, HNP, and HNP-VD) were incubated with the B16 melanoma line, and the MTT assay was performed after 24 hours. After this period, the viability protocol was performed as described in the methodology, and results were expressed as a percentage relative to the untreated control. As depicted in Figure 7, cell viability was not altered with all the formulations tested, although it was observed a reduction of viable cells at the highest nanoparticle concentration (500 μg/mL) for HNP and HNP-VD, but the results were not statistically significant. Notably, cells incubated with the HNP-VD formulation at 50 μg/mL exhibited a significant increase in viability after 24 hours, indicating cell proliferation. Previous study has shown that the activation of VD-VDR can promote a proliferation stimulus to melanoma cells[37]. The results obtained here indicated HNP-VD formulation as an important drug delivery system in melanoma cells.

Cells were maintained under optimal culture conditions for 24 hours under treatment. After this period, the viability

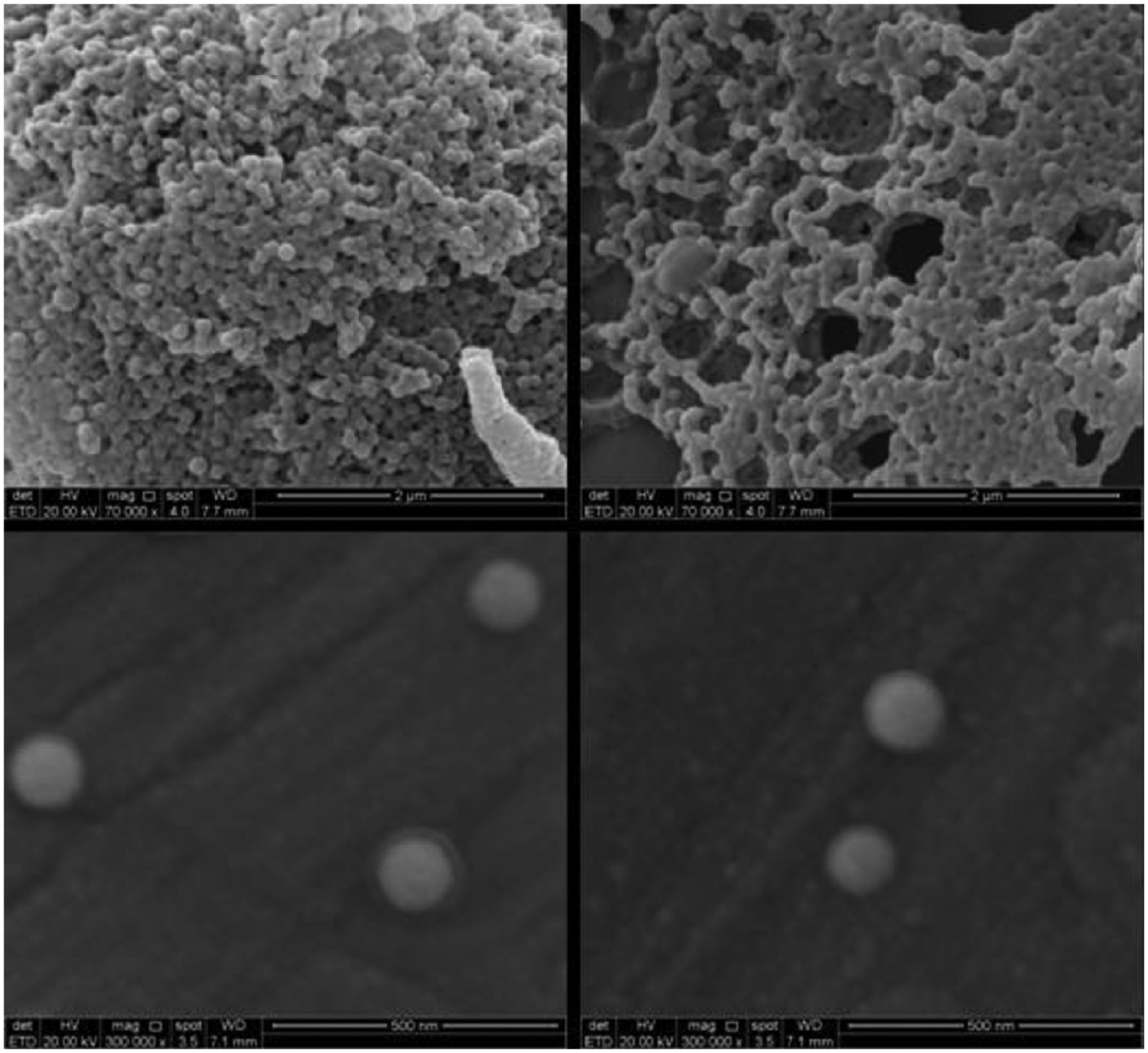

Figure 5. FEG-SEM images from HNPs (left) and HNP-VD (right) synthesized with the optimized lipid:NP ratio (1:25).

Table 6. Characterization of the NPs, HNPs, and HNP-VDs containing fluorescein.

	Size (nm)	PDI	Zeta potential (mV)	Drug loading (%)	Encapsulation efficiency (%)
NPs	170.33 ± 5.10	0.209 ± 0.006	−15.47 ± 0.37	2.72 ± 0.09	54.30 ± 1.90
NPHs	184.97 ± 4.45	0.236 ± 0.012	−18.30 ± 0.10	3.06 ± 0.08	61.20 ± 1.70
NPHs-F	230.10 ± 4.14	0.232 ± 0.011	−19.20 ± 0.20	3.22 ± 0.49	64.40 ± 9.70

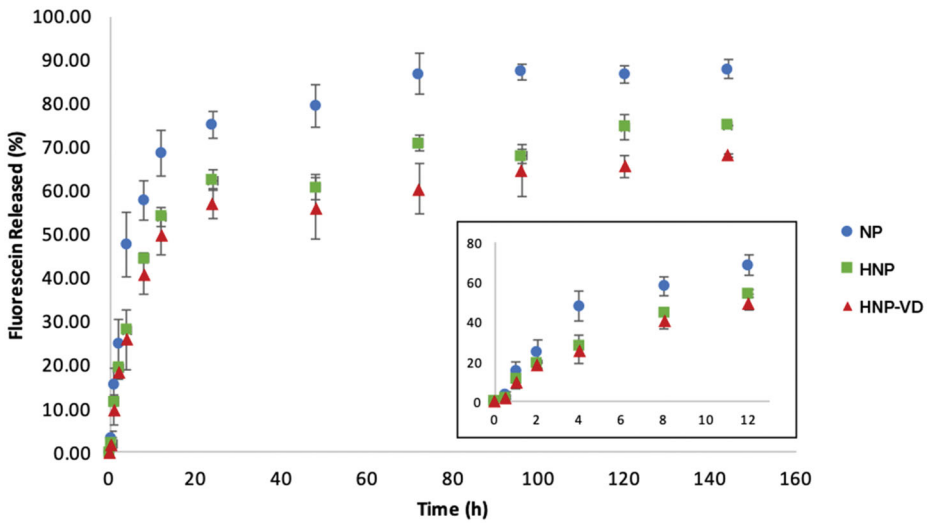

Figure 6. Fluorescein release behavior in PBS (pH 7.4; 0.01 M; 32.0°C) for the different samples.

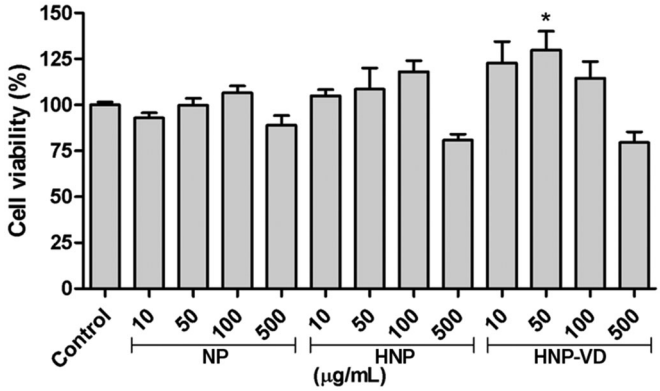

Figure 7. Evaluation of the cellular viability of B16 cells after treatment with NP, HNP and HNP-VD formulations at concentrations of 10, 50, 100 and 500 μg/mL.

protocol was performed as described in the methodology. The results are expressed as a percentage relative to the untreated control. The experiments were performed three times in triplicate.

3.5. Cellular uptake study

Nanoparticle uptake by melanoma cells was evaluated using fluorescence microscopy. After 3 hours of incubation with different formulations, it was observed that there was a difference in the cellular distribution of the nanoparticles according to their specific formulation (Figure 8). NP (A) and HNP (B) were located closer to the membrane of cells with decreased cytoplasmic distribution. Conversely,

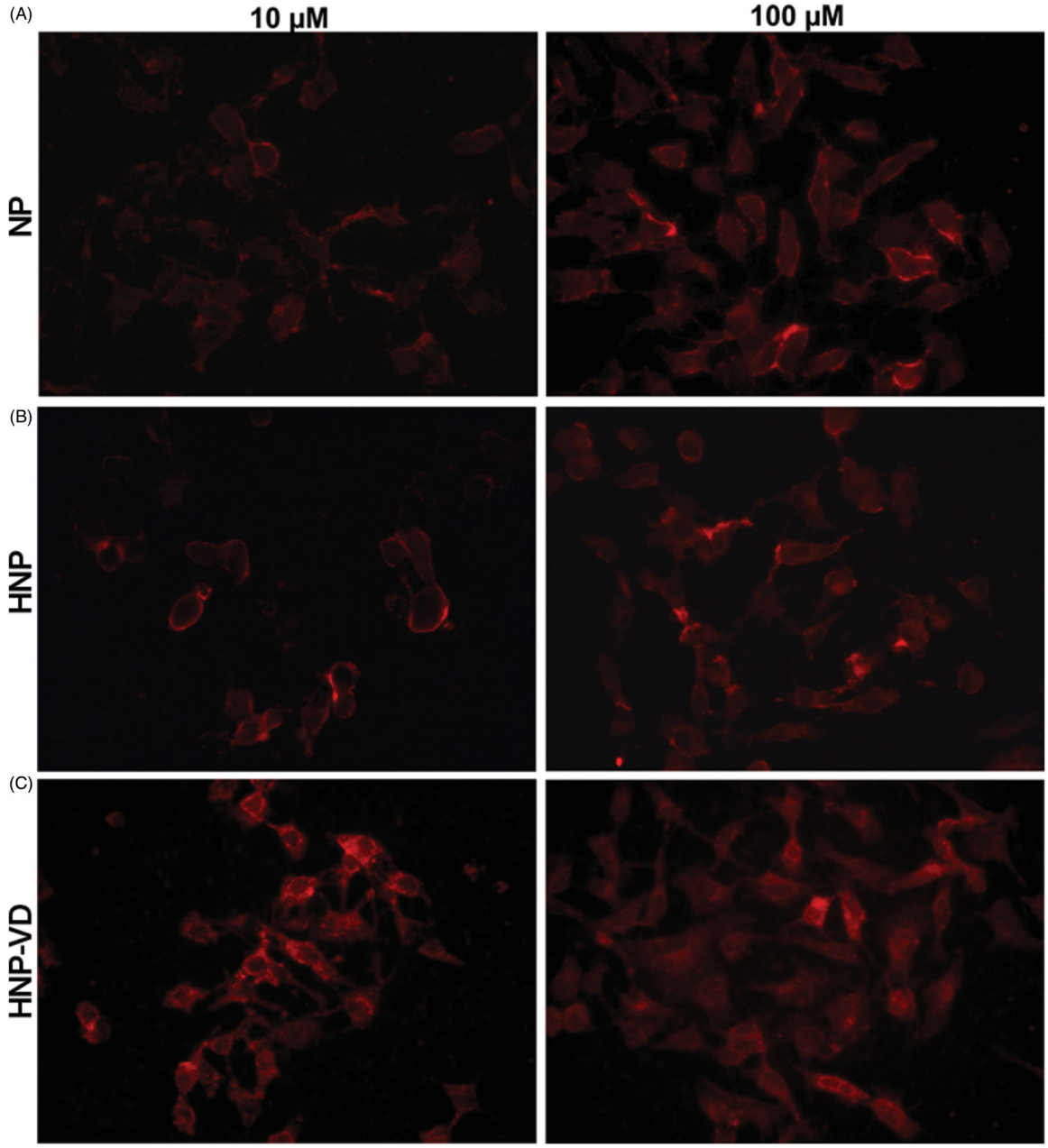

Figure 8. Cellular uptake by fluorescence microscopy.

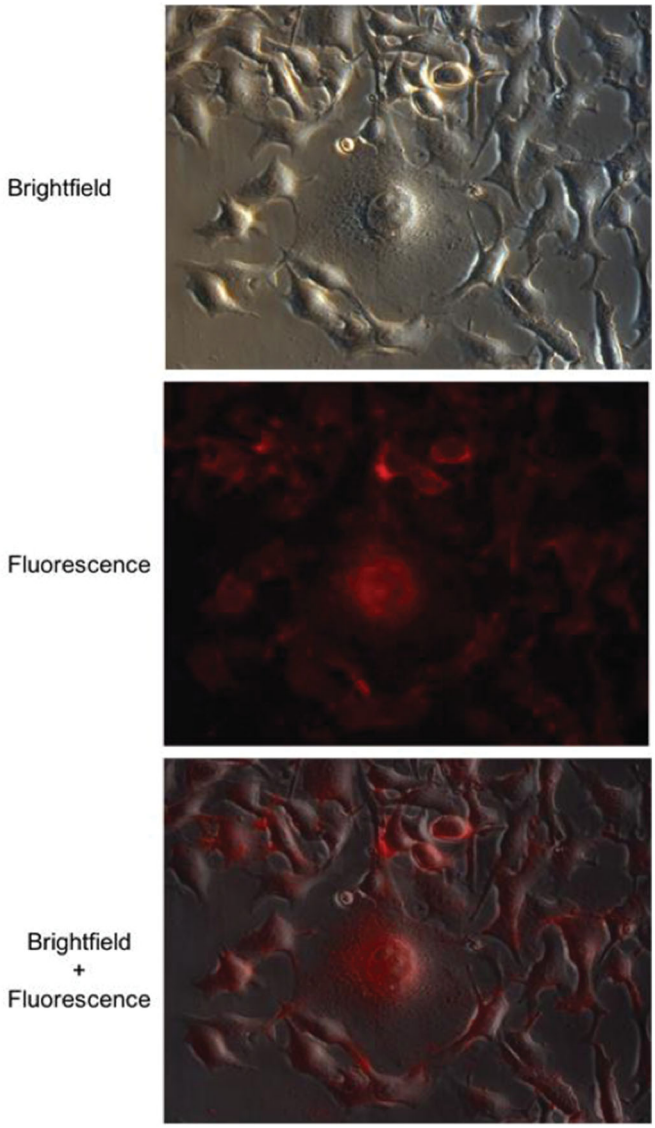

Figure 9. Cellular uptake and localization of HNP-VDs at the concentration of 100 μg/mL. The images were obtained from an objective with magnification of 400×.

HNP-VD (C) had more prominent localization in the cytoplasmic and perinuclear domains, as shown in Figure 8.

After the incubation with the different nanoparticle formulations (NP, HNP and HNP-VD) at concentrations of 10 and 100 μg/mL, the cells were maintained under optimum culture conditions for 3 hours and the fluorescence intensity was evaluated by an inverted microscope. The images were obtained from an objective with a 40x magnification. In order to facilitate the visualization of the proximity of HNP-VD to the nucleus of B16 melanoma cells, Figure 9 shows the images obtained by brightfield and fluorescence microscopy, and also the merged image using a larger magnification (400×). The images obtained here clearly showed that the HNP-VD nanoparticles were localized adjacent to the nucleus of melanoma cells. This indicates that HNP-VD nanoparticles may be well-suited to deliver therapeutics to the cell nucleus. Other studies have shown the benefit of the internalization of NPs by tumor cells. Almouazen et al.[38] showed that the uptake of Nile Red-labeled-NP by breast cancer MCF-7 cells improved the intracellular delivery of the encapsulated drug.

4. Conclusions

This work presents the synthesis of lipid-nanoparticle hybrids, with (HNP-VDs) and without (HNPs) a targeting receptor in the surface. The mass ratio of lipid:NP was optimized in order to obtain the optimal amount of lipids on the surface of the nanoparticles. According to the colorimetric method and the ^{1}H-NMR analysis, HNPs were produced with 97% of their surface area covered by the lipid layer. *In vitro* release of fluorescein showed an initial burst release of 75, 62, and 57% during the first 24 h for NPs, HNP, and HNP-VD, respectively, followed by a slower release for the remaining time period. These results indicate that the nanocarriers developed in this work can be used as controlled drug delivery systems for substances containing physicochemical properties similar to fluorescein. Moreover, we can conclude that the NPs and HNP did not promote significant effects on melanoma B16 cells, however, HNP-VD lead to an increase of cell proliferation, probably due the interaction VD-VDR. Cellular uptake data indicated that HNP-VD was concentrated in the perinuclear region of B16 melanoma cells, presumably due to the presence of the ligand vitamin D which targets nuclear receptor VDR. These results confirm that HNP-VD is a good candidate for the development of targeted melanoma treatment protocols as well as the specific delivery of encapsulated therapeutic agents to other cells containing nuclear vitamin D receptors.

Acknowledgments

The authors are grateful to the National Council for Scientific and Technological Development (*CNPq*) and Coordination for the Improvement of Higher Education Personnel (*CAPES*) for the Science without Borders Scholarship.

Funding

This work was supported by Conselho Nacional de Desenvolvimento Científico e Tecnológico; Coordenação de Aperfeiçoamento de Pessoal de Nível Superior.

ORCID

Fernanda B. Morrone http://orcid.org/0000-0002-2709-2801
Eduardo Cassel http://orcid.org/0000-0001-8843-0694
Rubem M. F. Vargas http://orcid.org/0000-0003-2696-8581

References

[1] Krishnamurthy, S.; Vaiyapuri, R.; Zhang, L.; Chan, J. M. Lipid-Coated Polymeric Nanoparticles for Cancer Drug Delivery. Biomater. Sci. **2015**, *3*, 923–936. DOI: 10.1039/C4BM00427B.
[2] Hadinoto, K.; Sundaresan, A.; Cheow, W. S. Lipid-Polymer Hybrid Nanoparticles as a New Generation Therapeutic Delivery Platform: A Review. *Eur. J. Pharm. Biopharm.* **2013**, *85*, 427–433. DOI: 10.1016/j.ejpb.2013.07.002.
[3] Sun, X.; Dong, S.; Li, X.; Yu, K.; Sun, F.; Lee, R. J.; Li, Y.; Teng, L. Delivery of siRNA Using Folate Receptor-Targeted pH-

Sensitive Polymeric Nanoparticles for Rheumatoid Arthritis Therapy. *Nanomed. Nanotechnol.* **2019**, *20*, 1–11.

[4] Dasa, S. S. K.; Suzuki, R.; Mugler, E.; Chen, L.; Jansson-Lofmark, R.; Michaelsson, E.; Lennart, L.; Klibanov, A. L.; French, B. A.; Kelly, K. A. Evaluation of Pharmacokinetic and Pharmacodynamic Profiles of Liposomes for the Cell Type-Specific Delivery of Small Molecule Drugs. *Nanomedicine.* **2017**, *13*, 2565–2574. DOI: 10.1016/j.nano.2017.07.005.

[5] Pandita, D.; Kumar, S.; Lather, V. Hybrid Poly(Lactic-co-Glycolic Acid) Nanoparticles: Design and Delivery Prospectives. *Drug Discov. Today.* **2015**, *20*, 95–104. DOI: 10.1016/j.drudis.2014.09.018.

[6] Kong, S. D.; Sartor, M.; Hu, C.-M. J.; Zhang, W.; Zhang, L.; Jin, S. Magnetic Field Activated Lipid-Polymer Hybrid Nanoparticles for Stimuli-Responsive Drug Release. *Acta Biomater.* **2013**, *9*, 5447–5452. DOI: 10.1016/j.actbio.2012.11.006.

[7] Gowda, R.; Dinavahi, S. S.; Iyer, S.; Banerjee, S.; Neves, R.; Pameijer, C. R.; Robertson, G. P. Nanoliposomal Delivery of Cytosolic Phospholipase A_2 Inhibitor Arachidonyl Trimethyl Ketone for Melanoma Treatment. *Nanomedicine.* **2018**, *14*, 863–873. DOI: 10.1016/j.nano.2017.12.020.

[8] Amoabediny, G.; Haghiralsadat, F.; Naderinezhad, S.; Helder, M. N.; Akhoundi Kharanaghi, E.; Mohammadnejad Arough, J.; Zandieh-Doulabi, B. Overview of Preparation Methods of Polymeric and Lipid-Based (Niosome, Solid Lipid, Liposome) Nanoparticles: A Comprehensive Review. *Int J. Polym Mater Po.* **2018**, *67*, 383–400. DOI: 10.1080/00914037.2017.1332623.

[9] Zhao, P.; Wang, H.; Yu, M.; Liao, Z.; Wang, X.; Zhang, F.; Ji, W.; Wu, B.; Han, J.; Zhang, H.; et al. Paclitaxel Loaded Folic Acid Targeted Nanoparticles of Mixed Lipid-Shell and Polymer-Core: *In Vitro* and *in Vivo* Evaluation. *Eur. J. Pharm. Biopharm.* **2012**, *81*, 248–256. DOI: 10.1016/j.ejpb.2012.03.004.

[10] Desai, P. R.; Marepally, S.; Patel, A. R.; Voshavar, C.; Chaudhuri, A.; Singh, M. Topical Delivery of anti-TNFα siRNA and Capsaicin via Novel Lipid-Polymer Hybrid Nanoparticles Efficiently Inhibits Skin Inflammation *in Vivo*. *J. Control. Release.* **2013**, *170*, 51–63. DOI: 10.1016/j.jconrel.2013.04.021.

[11] Mandal, B.; Bhattacharjee, H.; Mittal, N.; Sah, H.; Balabathula, P.; Thoma, L. A.; Wood, G. C. Core-Shell-Type Lipid-Polymer Hybrid Nanoparticles as a Drug Delivery Platform. *Nanomedicine.* **2013**, *9*, 474–491. DOI: 10.1016/j.nano.2012.11.010.

[12] Hu, Y.; Hoerle, R.; Ehrich, M.; Zhang, C. Engineering the Lipid Layer of lipid-PLGA Hybrid Nanoparticles for Enhanced *in Vitro* Cellular Uptake and Improved Stability. *Acta Biomater.* **2015**, *28*, 149–159. DOI: 10.1016/j.actbio.2015.09.032.

[13] Crucho, C. I. C.; Barros, M. T. Formulation of Functionalized PLGA Polymeric Nanoparticles for Targeted Drug Delivery. *Polymer.* **2015**, *68*, 41–46. DOI: 10.1016/j.polymer.2015.04.083.

[14] Baghaei, B.; Jafari, S. H.; Khonakdar, H. A.; Saeb, M. R.; Wagenknecht, U.; Heinrich, G. A Multioptimization Approach to Assessment of Drug Delivery of PLGA Nanoparticles: Simultaneous Control of Particle Size and Release Behavior. *Int J. Polym Mater Po.* **2015**, *64*, 641–652. DOI: 10.1080/00914037.2014.996714.

[15] Palange, A. L.; Mascolo, D. D.; Carallo, C.; Gnasso, A.; Decuzzi, P. Lipid-Polymer Nanoparticles Encapsulating Curcumin for Modulating the Vascular Deposition of Breast Cancer Cells. *Nanomedicine.* **2014**, *10*, 991–1002.

[16] Hu, Y.; Ehrich, M.; Fuhrman, K.; Zhang, C. *In Vitro* Performance of Lipid-PLGA Nanoparticle as an Antigen Delivery System: Lipid Composition Matters. *Nanoscale Res. Lett.* **2014**, *9*, 434. DOI: 10.1186/1556-276X-9-434.

[17] Mo, L.; Song, J. G.; Lee, H.; Zhao, M.; Kim, H. Y.; Lee, Y. J.; Ko, H. W.; Han, H. K. PEGylated Hyaluronic Acid-Coated Liposome for Enhanced *in Vivo* Efficacy of Sorafenib via Active Tumor Cell Targeting and Prolonged Systemic Exposure. *Nanomedicine.* **2018**, *14*, 557–567. DOI: 10.1016/j.nano.2017.12.003.

[18] Pettijohn, E.; Martone, B.; Rademaker, A.; Kuzel, T. A Phase I Study of High-Dose Calcitriol in Combination with Temozolomide for Patients with Metastatic Melanoma. *J. Pers. Med.* **2014**, *4*, 448–458. DOI: 10.3390/jpm4040448.

[19] Mason, R.; Pryke, A.; Ranson, M.; Thomas, H.; Posen, S. Human Melanoma Cells: Functional Modulation by Calciotropic Hormones. *J. Invest. Dermatol.* **1988**, *90*, 834–840. DOI: 10.1111/1523-1747.ep12462072.

[20] Slominski, A. T.; Janjetovic, Z.; Kim, T. K.; Wright, A. C.; Grese, L. N.; Riney, S. J.; Nguyen, M. N.; Tuckey, R. C. Novel Vitamin D Hydroxyderivatives Inhibit Melanoma Growth and Show Differential Effects on Normal Melanocytes. *Anticancer Res.* **2012**, *32*, 3733–3742.

[21] Hosoi, J.; Abe, E.; Suda, T.; Kuroki, T. Regulation of Melanin Synthesis of B16 Mouse Melanoma Cells by 1α, 25-Dihydroxyvitamin D3 and Retinoic Acid. *Cancer Res*, **1985**, *45*, 1474–1478.

[22] Verderio, P.; Bonetti, P.; Colombo, M.; Pandolfi, L.; Prosperi, D. Intracellular Drug Release from Curcumin-Loaded PLGA Nanoparticles Induces G2/M Block in Breast Cancer Cells. *Biomacromolecules.* **2013**, *14*, 672–682. DOI: 10.1021/bm3017324.

[23] Liang, X. F.; Wang, H. J.; Luo, H.; Tian, H.; Zhang, B. B.; Hao, L. J.; Teng, J. I.; Chang, J. Characterization of Novel Multifunctional Cationic Polymeric Liposomes Formed from Octadecyl Quaternized Carboxymethyl Chitosan/Cholesterol and Drug Encapsulation. *Langmuir.* **2008**, *24*, 7147–7153. DOI: 10.1021/la703775a.

[24] Wang, H.; Zhao, P.; Su, W.; Wang, S.; Liao, Z.; Niu, R.; Chang, J. PLGA/Polymeric Liposome for Targeted Drug and Gene Co-Delivery. *Biomaterials.* **2010**, *31*, 8741–8748. DOI: 10.1016/j.biomaterials.2010.07.082.

[25] Wang, H.; Wang, S.; Liao, Z.; Zhao, P.; Su, W.; Niu, R.; Chang, J. Folate-Targeting Magnetic Core-Shell Nanocarriers for Selective Drug Release and Imaging. *Int. J. Pharm.* **2012**, *430*, 342–349. DOI: 10.1016/j.ijpharm.2012.04.009.

[26] Pastorino, F.; Brignole, C.; Di Paolo, D.; Nico, B.; Pezzolo, A.; Marimpietri, D.; Pagnan, G.; Piccardi, F.; Cilli, M.; Longhi, R.; et al. Vascular Damage and anti-Angiogenic Effects of Tumor Vessel-Targeted. *Cancer Res.* **2006**, *66*, 10073–17409. DOI: 10.1158/0008-5472.CAN-06-2117.

[27] Massoumi, B.; Ghamkhari, A.; Agbolaghi, S. Dual Stimuli-Responsive Poly(Succinyloxyethylmethacrylate-b-N-Isopropylacrylamide) Block Copolymers as Nanocarriers and Respective Application in Doxorubicin Delivery. *Int J. Polym Mater Po.* **2018**, *67*, 101–109. DOI: 10.1080/00914037.2017.1300901.

[28] Yang, Z.; Luo, X.; Zhang, X.; Liu, J.; Jiang, Q. Targeted Delivery of 10-Hydroxycamptothecin to Human Breast Cancers by Cyclic RGD-Modified Lipid-Polymer Hybrid Nanoparticles. *Biomed. Mater.* **2013**, *8*, 025012. DOI: 10.1088/1748-6041/8/2/025012.

[29] Stewart, J. C. M. Colorimetric Determination of Phospholipids with Ammonium Ferrothiocyanate. *Anal. Biochem.* **1980**, *104*, 10–14. DOI: 10.1016/0003-2697(80)90269-9.

[30] Contri, R.; Kaiser, M.; Poletto, F.; Pohlmann, A.; Guterres, S. Simultaneous Control of Capsaicinoids Release from Polymeric Nanocapsules. *J. Nanosci. Nanotech.* **2011**, *11*, 2398–2406. DOI: 10.1166/jnn.2011.3521.

[31] Hara, K.; Tsujimoto, H.; Huang, C. C.; Kawashima, Y.; Ando, R.; Kusuoka, O.; Tamura, K.; Tsutsumi, M. Ultrastructural and Immunohistochemical Studies on Uptake and Distribution of FITC-Conjugated PLGA Nanoparticles Administered Intratracheally in Rats. *J. Toxicol. Pathol.* **2012**, *25*, 19–26. DOI: 10.1293/tox.25.19.

[32] Gehring, M. P.; Pereira, T. C. B.; Zanin, R. F.; Borges, M. C.; Filho, A. B.; Battastini, A. M. O.; Bogo, M. R.; Lenz, G.; Campos, M. M.; Morrone, F. B. P2X7 Receptor Activation Leads to Increased Cell Death in a Radiosensitive Human

Glioma Cell Line. *Purinergic Signal.* **2012**, *8*, 729–739. DOI: 10.1007/s11302-012-9319-2.

[33] Mccall, R. L.; Rebecca, L.; Sirianni, R. W. PLGA Nanoparticles Formed by Single- or Double-Emulsion with Vitamin E-TPGS. *J. Vis. Exp.* **2013**, *82*, 1–8.

[34] Fonte, P.; Soares, S.; Costa, A.; Andrade, J. C.; Seabra, V.; Reis, S.; Sarmento, B. Effect of Cryoprotectants on the Porosity and Stability of Insulin-Loaded PLGA Nanoparticles After Freeze-Drying. *Biomatter.* **2012**, *2*, 329–339. DOI: 10.4161/biom.23246.

[35] Mandal, B.; Mittal, N. M.; Balabathula, P.; Thoma, L. A.; Wood, G. C. Development and *in Vitro* Evaluation of Core-Shell Type Lipid-Polymer Hybrid Nanoparticles for the Delivery of Erlotinib in Non-Small Cell Lung Cancer. *Eur. J. Pharm. Sci.* **2016**, *81*, 162–171. DOI: 10.1016/j.ejps.2015.10.021.

[36] Zhang, L.; Chan, J. M.; Gu, F. X.; Rhee, J.-W.; Wang, A. Z.; Radovic-Moreno, A. F.; Alexis, F.; Langer, R.; Farokhzad, O. C. Self-Assembled Lipid – Polymer Hybrid Nanoparticles: A Robust Drug Delivery Platform. *ACS Nano.* **2008**, *2*, 1696–1702. DOI: 10.1021/nn800275r.

[37] Almouazen, E.; Bourgeois, S.; Jordheim, L. P.; Fessi, H.; Briancon, S. Nano-Encapsulation of Vitamin D3 Active Metabolites for Application in Chemotherapy: Formulation Study and *in Vitro* Evaluation. *Pharm. Res.* **2013**, *30*, 1137–1146. DOI: 10.1007/s11095-012-0949-4.

[38] Muralidhar, S.; Filia, A.; Nsengimana, J.; Poźniak, J.; O'Shea, S. J.; Diaz, J. M.; Harland, M.; Randerson-Moor, J. A.; Reichrath, J.; Laye, J. P.; et al. Vitamin D-VDR Signaling Inhibits Wnt/Beta-Catenin-Mediated Melanoma Progression and Promotes Anti-Tumor Immunity. *Cancer Res.* **2019**, *79*, 5986–5998. DOI: 10.1158/0008-5472.CAN-18-3927.